

# **AUTOMATIC GEOMETRIC AND RADIOMETRIC REGISTRATION OF LANDSAT-TM IMAGES USING MUTUAL INFORMATION**

J.P. Queiroz-Neto, M. F.M. Campos, B. W. Nelson, J. L. S. Pio  
*CEFET - CEFET/AM--Centro Federal de Educação Tecnológica do Amazonas,UFMG -  
Universidade Federal de Minas Gerais, INPA - Instituto Nacional de Pesquisas da Amazônia.  
UFAM - Universidade Federal do Amazonas,*

**Abstract:** This work is on development of a method for automatic registration of satellite images acquired on different dates, for both geometric and radiometric correction with respect to a reference image. Mutual information statistics is used as the similarity metric of geometric and radiometric registration. Affine and linear transformations are used in geometric and radiometric correction respectively. Powell's method is applied in iterative optimization to find the best transformation parameters for both types of registration, based on the maximum mutual information between images. The method is validated using Landsat's Thematic Mapper (TM) sensor, bands 3, 4 and 5 images, obtained on five separate dates for scene 231-062 in the Central Amazon.

**Key words:** radiometric registration, geometric registration, mutual information.

## **1. INTRODUCTION**

Environmental research makes significant use of satellite images of forest. Among the most commonly available orbital sensor images are those acquired by Landsat-TM. Studies requiring change detection between images acquired at distinct times have been a difficult task for researchers, mainly because of problems arising from geometric and radiometric distortions inherent in the acquisition system and temporally variable atmosphere. Without registration, programs to produce and analyze data

from the same region will have inaccurate results, because pixels that represent a given target will not be in the same image positions, and areas will have different radiometric values.

Currently, image registration of orbital sensor images is accomplished with the aid of user defined control points on both the reference and subject images. The majority of methods only correct the geometry of the image. Use of control points in a time series of forested areas presents specific challenges and limitations. A control point taken in a reference image, which corresponds to a given feature in the scene, may not be visible in all images of the series, either due to natural changes in that region, or because of human interference. Moreover, it is difficult to obtain control points in areas like the Amazon.

Forest, which typically has extensive areas of dense homogeneous vegetation cover, oftentimes without distinguishable features like roads, constructions or anything that could be considered an immutable control point.

This work aims at studying and implementing a methodology to automate registration of multi-temporal images to for orbital sensors in general, but more specifically it was tested with Landsat-TM images, correcting both geometric and radiometric distortions. The latter receive greater emphasis. Section 2 defines the problem and how it has been dealt with in the literature. We then show in Section 3 how Mutual Information may be used as a similarity metric. Geometric and Radiometric Transformation functions are discussed in Section 4 and in Section 5 an optimization method to recover geometric and radiometric parameters is explained. Finally the results obtained by applying these methods to Landsat time series of a given area of Amazon Forest and a discussion of their quality are covered in Sections 6 and 7.

## **2. PROBLEM DEFINITION AND PREVIOUS WORK**

The problem of geometrically and radiometrically registering two or more images of the same orbital sensor scene can be thought of as an overlay operation such that each pair of overlapping points is made to correspond to the same true point of the real landscape [Fonseca, 1999] with the brightness of the pixel at that point being made constant if it has undergone no natural or human-induced change.

Geometric distortions can be caused by position, size and orientation of a pixel to be altered during the acquisition process. The causes of such geometric errors include Earth rotation during the acquisition process, land

curvature, platform speed and altitude variations, changes in topographical elevation, sensor's parameters, among others [Fonseca, 1999].

The radiometric distortions affect pixel-encoded radiance and are mainly caused by atmospheric conditions, scene illumination, sensor gains and satellite observation angles at the moment of the image acquisition [Hal et al., 1991].

In manual methods, control points common to all images are carefully selected for the geometric registration via a polynomial transformation [Brown, 1992]. This approach is tedious and time-consuming and commonly introduces modeling errors, since the most reliable points may not be uniformly distributed.

Area-based methods are used when the images have not prominent details and the distinctive information is provided by graylevels/colors rather than local shapes and structure [Zitova and Flusser, 1993]. This method uses correlation measures, including mutual information, but just to geometric registration.

[Fonseca 1999, 1996] developed an automatic method of geometric registration, where candidate control points are extracted using the local maxima of the wavelet coefficients. Search for control points starts in the lowest resolution of the wavelet decomposition and is refined at progressively higher resolutions. The method uses a correlation coefficient as a similarity metric for control point selection. This method was applied in [Fedorov et al., 2003] to develop an automatic registration and mosaicking system with good results; however, according to the author, it has limitations when applied in uniformly dense vegetation areas. Samadzadegan [Samadzadegan et al., 2003] uses the same logic in a genetic algorithm to identify and compare such features as corners, intersections and centers of gravity.

Viola [Viola, 1995] and Collingnon et al. [Collingnon et al., 1995] independently proposed a method for automatic geometric registration of medical images, using mutual information to measure statistical dependence between two random variables or the amount of information that one variable contains about another. The registration criterion states that the mutual information of the image intensity values of corresponding points is maximal if the images are geometrically aligned. The method assumes that the intensities of the two images are linearly correlated, but does not address radiometric distortions, because medical images are acquired under controlled conditions. Orbital sensor images of the same scene acquired on two different dates generally will show radiometric differences condition due to less controlled conditions as noted above.

Absolute radiometric restoration of a time series of images from an optical orbital sensor would be a difficult task, because it would be necessary to know all the conditions which influence radiometric distortion, between

all the subject images, such as the sun's inclination angle, atmospheric conditions, sensor view angle and sensor gain. Such information may be unavailable for images 10 or 20 years old, or images acquired by different institutions, yet are necessary to evaluate landscape change in a multi-temporal series. Different from absolute radiometric restoration, the radiometric correction will calibrate all the subject images to the same reference image's radiometric conditions, but will not necessarily correct distortions from turbulence blur, aerosol blur, or path radiance.

Elvidge [Elvidge et al., 1995] , Hall [Hall et al., 1991] and other researchers [Schott et al., 1988; Heo and FitzHugh, 2000] propose what they call radiometric normalization between reference and subject images. Their methods use linear regression between pixel values from temporally stable water (low radiance) and built-up areas (high radiance). From these unchanging pixels they obtain a linear transformation and apply it to all subject image pixels, thereby calibrating them to the reference image. This method gives good results but has serious limitations due to the limited types of features taken to be reliably stable reference pixels.

[Song et al., 2003] use the unique spectral signature of water pixels in satellite images and apply a radiative transfer model to a variety of clear-sky conditions to generate functional relationships between the radiation due to the atmospheric scattering above water bodies and atmospheric radiative properties. The method requires water bodies in the scene. The use of filters, like atmospheric Wiener filter and Kalman filter [Arbel et al., 2004] can correct radiometric distortions for turbulence blur, aerosol blur, and path radiance simultaneously, but require meteorological data.

Some studies address only geometric correction of images while others consider only radiometric restoration or radiometric correction, assuming images to be geometrically corrected. This limitation is described by the *Correspondence Problem*, that can be represented by:

$$S(x',y')=G(R(T(x,y))), \quad (1)$$

where  $R$  and  $S$  are, respectively, the reference and subject images to be registered,  $T$  is a 2D geometric transformation function that maps a point coordinate with  $x$  and  $y$ , into a point of co-ordinates  $x'$  and  $y'$ .  $G$  is the 1D radiometric transformation function. It is clear that there is an interdependence between functions. In other words, it is necessary to first geometrically correct an image then correct its radiometry. But on the other hand, to perform geometric correction without preprocessing the image, it is necessary use a radiometrically corrected image.

### 3. MUTUAL INFORMATION AS A SIMILARITY METRIC.

The origin of Mutual Information (MI) is credited to Shannon [Shannon, 1948] in his article published in 1948, where he explains many of its uses, including basic statistics, communication theory and complexity analysis [Egnal, 2000]. It was first and independently used for medical image registration in 1995 by [Viola, 1995] and [Collingnon et al., 1995]. Mutual information is related to entropy according to Equation [Maes et al., 1997]:

$$MI(A,B) = H(A) + H(B) - H(A,B), \quad (2)$$

$$MI(A,B) = H(A) - H(A|B), \quad (3)$$

$$MI(A,B) = H(B) - H(B|A), \quad (4)$$

where  $H(A)$  and  $H(B)$  are the entropy of  $A$  and  $B$ ,  $H(A,B)$  is their joint entropy and  $H(A|B)$  is the conditional entropy of  $A$  given  $B$ ; similarly  $H(B|A)$  is given by

$$\begin{aligned} H(A) &= -\sum_a P_A(a) \log P_A(a) \\ H(A,B) &= -\sum_{a,b} P_{A,B}(a,b) \log P_{A,B}(a,b) \\ H(A|B) &= -\sum_{a,b} P_{A,B}(a,b) \log P_{A|B}(a|b) \end{aligned} \quad (5, 6, 7)$$

Entropy  $H(A)$  indicates the uncertainty measure on the random variable  $A$ , while  $H(A|B)$  is uncertainty of  $A$  given  $B$ . Therefore,  $MI(A,B)$  from Equation 3 is uncertainty reduction in the random variable  $A$  from knowledge of another random variable  $B$ , or equivalently, a measure of information that  $B$  contains on  $A$ . Mutual information satisfies some important properties that can be seen in [Maes et al., 1997]. The interpretation of these properties confirms that the mutual information measures the degree of interdependence between two variables, reaching the lower bound when the two images are completely independent, and the upper bound when the images are the same.

Mutual information  $IM_{RS}$ , that expresses the similarity between a reference  $R$  and subject  $S$  images, defined from Equations 2, 5 and 6, is given by

$$IM_{RS}(r, s) = \sum_{r,s} P_{RS}(r, s) \log \left( \frac{P_{RS}(r, s)}{P_R(r)P_S(s)} \right), \quad (8)$$

where  $r$  and  $s$  are the pixel values from  $R$  and  $S$  images,  $P_R(r)$  and  $P_S(s)$  the probability distributions of  $r$  and  $s$  in each image, and  $P_{RS}(r,s)$  the joint probability distribution of  $r$  and  $s$ .

To calculate mutual information become necessary to know the probabilities  $P_R(r)$ ,  $P_S(s)$  and  $P_{RS}(r,s)$  both of them in Equation 8. These can be obtained estimating pixel value densities using histograms [Egnal, 2000].

The following procedures are executed to improve the efficiency of mutual information calculation between images [Machado, 1999]:

- The term  $\log(P_{RS}(r,s)/P_R(r).P_S(s))$  is decomposed in  $\log P_{RS}(r,s) - \log(P_R(r) - \log P_S(s))$ , and the logarithms' values are stored in tables. All the probability values have a factor  $1/n$  and they may be precomputed. The computational complexity is quadratic, but each term requires only one simple multiplication and two subtractions.
- LUTprob and LUTlog are auxiliary tables (lookup tables) where probabilities are derived from the histogram. Because they are calculated only once, there is an added memory cost of  $O(p*q)$  on the number of columns and rows in the image, which is acceptable considering the overall gain in efficiency.

$$LUTlog[i] = \log(i/n), LUTprob[i] = i/n. \quad (9)$$

#### 4. GEOMETRIC AND RADIOMETRIC TRANSFORMATION FUNCTIONS

Two transformation functions are used in this work, one applied to the geometric correction, and the other applied to the radiometric correction of the subject image  $S$ . When using mutual information, the best type of transformation indicated for the geometric registration of remote sensing images is the generic affine transformation, considering its computational efficiency.

In the generic affine transformation, angles and lengths can change but parallel lines continue parallel. This transformation allows shear in both  $x$

and  $y$  directions, and changes in aspect ratio. The 2D generic affine transformation function is given by Equation 10[Brown, 1992]:

$$\begin{bmatrix} x_2 \\ y_2 \end{bmatrix} = \begin{bmatrix} a & b \\ c & d \end{bmatrix} \begin{bmatrix} x_1 \\ y_1 \end{bmatrix} + \begin{bmatrix} e \\ f \end{bmatrix} \quad (10)$$

The transformation function has six parameters, two for rotation, two for translation and two for scale, denoted as  $a_x$ ,  $a_y$ ,  $b_x$ ,  $b_y$ ,  $c_x$ , and  $c_y$  respectively. In general,  $T(x,y)$  does not result in  $(x',y')$  pixel centers and orientations that coincide precisely with the pixel centers and orientations in the reference image, so an interpolation is necessary to get the pixel encoded radiance value  $r(x',y')$ . Among the wide variety of interpolation methods in remote sensing we chose to use the *Nearest Neighbor* as it preserves original pixel values of the subject image. This is an important feature considering the *Correspondence Problem* and the posterior application of a radiometric transformation.

When a sensor records the solar energy on Earth's surface, the atmosphere affects both the target radiance and irradiance. As sunlight pierces through the atmosphere, it is both attenuated and scattered, reducing target illumination and making it diffuse. The atmosphere also acts as a scattering reflector, adding extra radiance directed back to the sensor. When expressing these two atmospheric effects mathematically, the total radiance recorded for the sensor can be related to the object's reflectance at the surface and to the irradiance using the Equation 11 [Lillesand et al., 1987]:

$$L_{tot} = \frac{\rho ET}{\pi} + L_p. \quad (11)$$

where  $L_{tot}$  is the total radiance measured by the sensor,  $T$  the atmospheric transmittance and  $L_p$  the radiance of atmosphere the target to sensor trajectory (and not of the object) from the scattering effect. Rewriting Equation \ref{eq:rad0}:

$$L = K_1 \rho + K_2, \quad (12)$$

where  $L$  is the radiance at the sensor,  $\rho$  is the object reflectance,  $K_1$  is the constant that includes the solar irradiation, reflected radiance, and atmospheric transmission, and  $K_2$  describes the atmospheric path radiance. This form is presented in [Schott, 1988] as a viable expression for conditions where the sensor view angle is relatively narrow, as in Landsat-TM images. Moreover, for many sensors DN (Digital Number) in each band is simple a

linear function of irradiance at sensor. This is the case of Landsat-TM sensors [Markham and Barker, 1987], given by Equation 13:

$$DN = K_3L + K_4 \quad (13)$$

Where  $DN$  is the digital value proportional to total radiance detected at the sensor,  $K_3$  is a constant that incorporates the optic efficiency, detector response and gain, and  $K_4$  compensates dark current [Schott, 1988]. Combining Equations 12 and 13 in  $R$  and  $S$  images:

$$DN_R = m_R\rho_R + b_R, \quad DN_S = m_S\rho_S + b_S, \quad (14)$$

where  $DN_R$  and  $DN_S$  are the pixels' encoded radiance values on the two images,  $m_R$ ,  $m_S$ ,  $b_R$  and  $b_S$  are constants. For the same regions in two images that have not suffered natural or human alterations is possible to consider that  $\rho_R = \rho_S$ , and the pixel values of image  $S$  can be transformed to their values on image  $R$  using Equation 14, by:

$$DN_{S'} = \frac{m_R}{m_S} DN_S + b_R - \frac{m_R}{m_S} b_S \quad (15)$$

This expression can be simplified to:

$$G(DN_S) = ga * DN_S + of, \quad (16)$$

where  $G$  is the linear radiometric transformation function applied in registering image  $S$  to image  $R$ ,  $ga$  the gain and  $of$  the offset of this function, applied to every pixel in subject image  $S$ .

## 5. OPTIMIZATION METHOD TO RECOVER THE GEOMETRIC AND RADIOMETRIC PARAMETERS

Consider  $\alpha = (a_x, a_y, b_x, b_y, c_x, c_y, ga, of)$  the parameter set used for the five operations of image registration, being respectively the rotation, translation, scale, gain and offset parameters, as seen previously (Section 4), applied to image  $S$  using a transformation function  $T(\alpha)$  that includes geometric and radiometric transformations. The optimum parameters that lead to the registration are reached when the mutual information between the



reference and subject images is maximum. Testing all the possible parameters' values is impracticable due to low computational efficiency. Different from the gradient optimization method, this study uses a technique called *Direction Set Methods in Multidimensions* (Powell's Method) [Press et al., 1992], that requires only an evaluation of the  $T(\alpha)$  function. The logic is outlined in Figure 1. However, gradient-based methods such as the Gradient Conjugate or Levenberg-Marquardt could be implemented, as in [Viola, 1995].

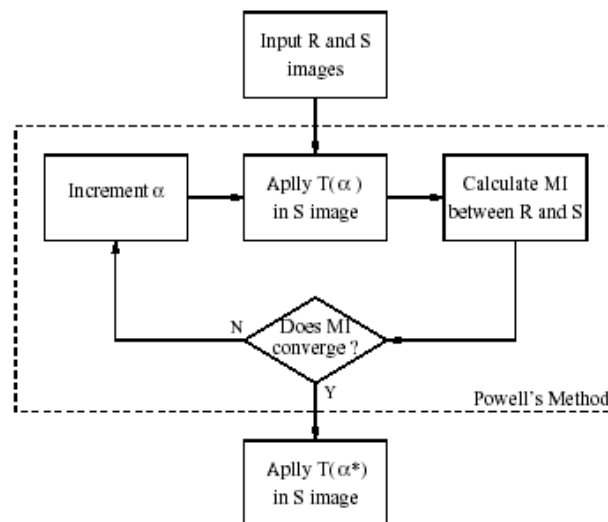


Figure 1. Program ARMI Fluxogram (Automatic Registration based in Mutual Information).

Powell's Method searches for the minima of  $N$  dimensions of the  $T(\alpha)$  through successive minimization. This is done one dimension at a time, through a set of  $M$  different directions, always initiating from the minimum found in the previous direction, and using a method of unidimensional minimization, such as Brent's Method. Registration is accomplished when the minima of  $T(\alpha)$  is found, always following the basic premise that this occurs at the state of maximum mutual information between the two images. Thus:

$$\alpha^* = \arg \min_{\alpha} IM_{RS}(\alpha), \quad (17)$$

where  $\alpha^*$  is the final parameter set used in  $T(\alpha^*)$  applied to  $S$  to obtain geometric and radiometric registration. Figure 1 shows the method as applied here and can be summarized in the following steps:

- Apply geometric and radiometric transformation function  $T(\alpha_{initial})$  to the subject image.
- Calculate the mutual information between reference and subject image using Equation 14.
- Use optimization search to find the best transformation parameters based on maximum mutual information between the images.
- Apply geometric and radiometric transformations to subject image using the parameters determined in previous step.

The method takes a long time to converge if the direction set and initial parameters are poor. The search efficiency can be improved with multi-resolution technique [Fonseca, 1999].

## 6. IMPLEMENTATION AND RESULTS

Implementation of ARMI (Automatic Registration based on Mutual Information) uses mutual information (Equation 8) as a similarity metric, the generic affine geometric transformation (Equation 10), a linear radiometric transformation (Equation 16) and Powell's Method (Section 5) in the search for optimum registration parameters.

The initial values of the parameter vector is very important, bearing a strong influence on the convergence time. An incorrect choice of these parameters implies longer search time, or even non-convergence, thus not allowing the registration. The initial parameter vector used here were obtained experimentally (data and graphics are show in [Queiroz-Neto, 2001] and are similar to those given by the Maes [Maes et al., 1997], resulting in  $\alpha_{initial} = (0.08, 0.08, 5.0, 5.0, 1.0, 1.0, 1.0, 0.0)$ , 5 degrees rotation, 5 pixels translation, spatial scaling of 1.0 and radiometric gain of 1.0. The set of initial directions is the identity matrix  $I_N$ , where  $N$  is the number of parameters ( $N=8$  in this study).

All experiments were executed on a Pentium 800MHz machine running Linux. The first experiment used two band 5 (middle infrared) images of Amazon forest with a "fish-spine" pattern of roads and their associated deforestation (Table 1). These are the same images used in [Fonseca, 1999], thus allowing a comparison with her results for the geometric registration. ARMI was applied and Table 2 presents geometric results. Figure 2 shows the resulting image.

Table 1. Reference and subject images used in first experiment.

<i>Image</i>	<i>Acquisition Date</i>	<i>Discrimination</i>
TM955AM	03/08/1995	reference image
TM975AM	07/07/1997	subject image

Table 2. Final geometric transformation parameters, divided in  $a_x$  and  $a_y$  (rotation in radians), ( $b_x$  and  $b_y$  (scale non dimensional) and  $c_x$  and  $c_y$  (translation in pixels).

<i>Image</i>	<i>Rotation</i>		<i>Scale</i>		<i>Translation</i>	
	$a_x$	$a_y$	$b_x$	$b_y$	$c_x$	$c_y$
TM975AM	0.00	0.00	0.99	1.01	45.43	15.93

In the second experiment, ARMI was used in multi-temporal images of Landsat-TM 231-062 scene (Figure 3) that encloses part of the state of Amazonas, using bands 3, 4 and 5, acquired on separate dates shown in Table 3.

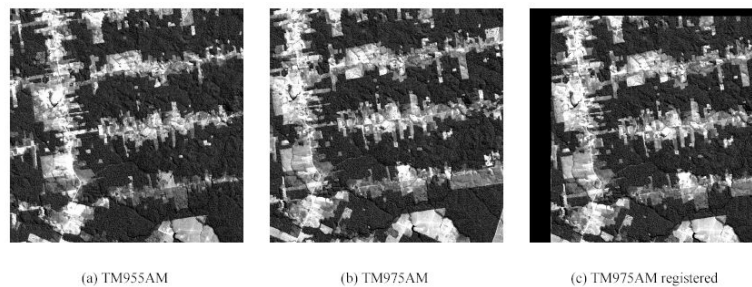


Figure 2: (a) and (b) the reference and subject images (kindly provided by Fonseca (INPE)). In (c) the subject registered image.

Table 3. Multi-temporal images of Landsat-TM 231\_062 scene used in ARMI.

<i>Acquisition Date</i>	<i>Discrimination</i>
06/07/1985	subject image 1
15/08/1988	subject image 2
21/08/1990	subject image 3
<b>03/08/1995</b>	<b>reference image</b>
15/09/1999	subject image 4

All images were kindly provided by the 4<sup>th</sup> Mapping Division of Brazilian Army. The 1995 reference image (Figure 3) is geo-referenced with 0.5 pixels average geometric error. For clarity of understanding, results are divided into geometric and radiometric registration parameters, as shown in Tables 4 and 5. Figure 4 shows the four subject images and registration results.

## 7. DISCUSSION

This work uses root mean square error (RMSE) [Queiroz-Neto, 2001] as an error measure, calculated differently for the geometric and radiometric registrations. In the first case, usually we use the same geometric control points for both the reference and registration images to determine the RMSE. As ARMI does not use control points, this work follows the procedure of [Trucco and Verri, 1998] requires a subjectively chosen set of verification points on the image for which RMSE is being calculated. Position units are in pixels. In [Maes, 1997a] 8 corresponding points pairs are marked in both the reference and registered images and used to calculate the error. Crosta [Crosta, 1993] suggests that 6 to 10 points are enough in images of 1000 by 1000 pixels when a generic affine transformation is used. A more refined statistical evaluation must be undertaken to verify if this amount of points is enough, but considering the good results obtained in [Maes, 1997a] this work uses 8 points distributed over each of the two images.

Table 4. Final geometric transformation parameters, divided in  $a_x$  and  $a_y$  (rotation in radians),  $b_x$  and  $b_y$  (scale non dimensional) and  $c_x$  and  $c_y$  (translation in pixels).

Image	Rotation		Scale		Translation	
	$a_x$	$a_y$	$b_x$	$b_y$	$c_x$	$c_y$
1985	-0.16	0.11	0.80	0.84	-13.04	-5.35
1988	-0.18	0.12	0.82	0.83	-4.20	-13.39
1990	-0.18	0.12	0.83	0.83	-8.71	-12.83
1999	-0.13	0.13	0.89	0.89	-4.30	-1.45

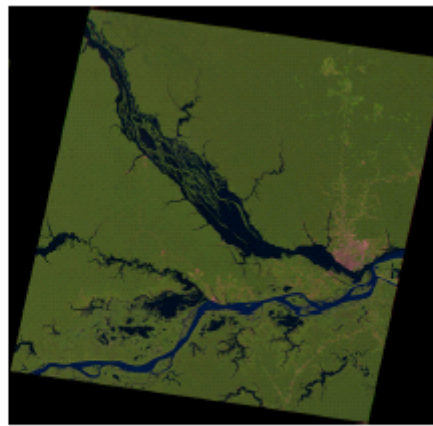


Figure 3. Reference image (1995) from Landsat-TM 231-062 scene.

Table 5. Final radiometric transformation parameters divided in  $ga$  (gain) and  $of$  (offset), both in units of encoded radiance.

Image	Band	$ga$	$of$
1985	3	1.009	-3.113
	4	1.020	-5.227
	5	0.997	-0.999
1988	3	0.716	1.032
	4	0.867	-1.892
	5	0.991	0.000
1990	3	0.793	-0.708
	4	0.888	-1.696
	5	0.981	0.618
1999	3	0.698	-0.142
	4	0.718	-0.281
	5	0.678	-0.002

To measure error of the radiometric registration, the method consists of identifying no change (NC) pixels that are taken to have been spectrally stable, without any natural or human-induced changes between the time when reference and subject images were acquired by the orbital sensor. Thus any spectral difference in the NC area between the two dates prior to registration will be attributable only to those effects being removed by the registration: atmosphere, illumination and sensor. A scattergram with a controlled linear regression defines this set of points automatically using bands 3 and 4 of the two images which are used in RMSE calculation, with units in uncorrected encoded radiance (DN). Let  $p_R(x_i, y_i)$  and  $p_S(x_i, y_i)$  be the pixel DN values at point  $(x_i, y_i)$  of the reference and registered image, both contained in the NC (no change) population. The radiometric RMSE is given by:

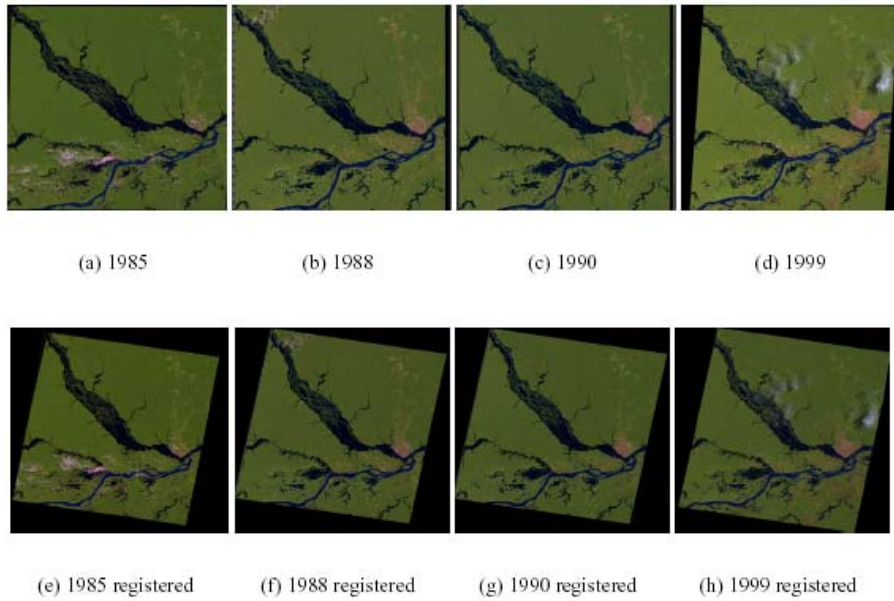


Figure 4. (a) to (d) the subject images and (e) to (f) the registration results.

$$RMSE_{RAD} = \sqrt{\frac{1}{NC} \sum_{i=1}^{NC} (p_{S(x_i, y_i)}^2 - p_{R(x_i, y_i)}^2)} \quad (18)$$

Table 6 presents the geometric error in the registered image of experiment one, comparing the proposed method (ARMI) and the method

described in [Fonseca, 1998] denoted AGRMR (Automatic Geometric Registration based on Multiple Resolution) in this study.

In experiment two, Table 7 presents geometric error in the registered images, but in this case is not compared with AGMR because we have no results using it in this images, and Table 8 presents the radiometric errors in DN's between reference and registered images, comparing with results using the radiometric normalization technique ASCR (Automatic Scattergram-Controlled Regression) from [Elvidge et al., 1995]. ASCR was applied to images with prior geometric registration, since, unlike ARMI, the technique does not perform geometric registration.

Table 6. Geometric registration error in pixels using ARMI and AGRMR.

<i>Imagem</i>	<i>(ARMI)</i>	<i>(AGRMR)</i>
TM975AM	0.756	0.665

Table 7. Geometric registration error in pixels.

<i>Image</i>	<i>RMSE<sub>Geo</sub></i>
1985	1.134
1988	0.926
1990	1.031
1999	0.935

Experiment one showed that ARMI performed with a geometric error of less than 1 pixel, while AGRMR obtained slightly better results. In the second experiment all the registered images presented a geometric error of about 1 pixel. This is a good result considering the limitations inherent in generic affine transformation. In the case of the radiometric correction, the result is compared with the ASCR technique. The two methods are basically the same with regards to errors. Thus, ARMI has proven to be good as another more established method, which justifies using the method proposed in this study.

Table 8. Radiometric registration error in DN's using ARMI and ASCR.

<i>Image</i>	<i>Band</i>	<i>ARMI</i>	<i>ASCR</i>
1985	3	2.026	2.106
	4	2.107	2.212
	5	2.306	2.486
1988	3	2.220	1.873
	4	2.691	2.568
	5	2.848	2.858
1990	3	3.521	2.413
	4	2.482	3.109
	5	3.563	3.150
1999	3	2.238	2.247
	4	2.769	2.825
	5	2.996	3.009

## 8. CONCLUSIONS

We present an automatic registration method for satellite images time series which is able to simultaneously correct both the geometric and radiometric distortions.

The method was used to register 5 images of scene 231-062, which covers an area of over 30000 km<sup>2</sup> covering Amazon forest, two large rivers and their tributaries. Experimental results were evaluated using root mean square error and the procedure described in [Trucco and Verri, 1998] for geometric registration and in [Elvidge et al., 1995] for radiometric registration. The method proved reliable, as shown by visual comparisons and the low RMSE values obtained.

Limitations of the method are the high computational cost and the need for minimum entropy between reference and subject, i.e., that there are large areas of no change. Future works are to introduce a multi-resolution technique to decrease computational cost while maintaining low RMSE.

## ACKNOWLEDGMENTS

This work would not have been possible without the financial support of CNPq. The authors also thank the Dr. Frederik Maes and Dr. Leila Fonseca for their valuable suggestions. Geo-referenced image used here was kindly provided by the 4th Mapping Division of the Brazilian Army.



## REFERENCES

- Arbel, D., Cohen, E., Citroen, M., Blumberg, D.G., and Kopeika, N.S. (2004). Landsat tm satellite image restoration using kalman filters. *Photogrammetric Engineering and Remote Sensing*, 70(1).
- Brown, L. G. (1992). A survey of images registration techniques. *ACM Computing Surveys*, 29:325–376.
- Collignon, A., Maes, F., Delaere, D., Vandermeulen, D., Suetens, P., and Masshal, G. (1995). Automated multi-modality image registration based on information theory. In Academic, Kluwer, editor, *In information processing in medical imaging 1995*, pages 263–274.
- Crosta, A. P. (1993). *Processamento Digital de Imagens*. IG/UNICAMP.
- Egnal, G. (2000). Image registration using mutual information. *Computer and Information Science MS-CIS-00-05*.
- Elvidge, C. D., Yuan, D., Weerackoon, R. D., and Lunetta, R. S. (1995). Radiometric normalization of landsat multispectral scanner (mss) data using an automatic scattergram-controlled regression. *Photogrammetric Engineering and Remote Sensing*, 61(10):1255–1260.
- Fedorov, D., Fonseca, L. M. G., Kenney, C., and Manjunath, B. S. (2003). Automatic registration and mosaicking system for remotely sensed imagery. In Serpico, S. B., editor, *Proceedings of SPIE*.
- Fonseca, L. M. G. (1999). Registro Automático de Imagens de Sensoriamento Remoto Baseado em Múltiplas Resoluções. PhD thesis, Instituto Nacional de Pesquisas Espaciais.
- Fonseca, L. M. G. and Manjunath, B. S. (1996). Registration techniques for multisensor remotely sensed images. *Photogrammetric Engineering and Remote Sensing*, 62(9).
- Hall, F. G., Strebel, E. D., Nickeson, J. E., and Goetz, S. J. (1991). Radiometric rectification: Toward a common radiometric response among multitemporal, multisensor images. *Remote Sensing of Environments*, 35:11–27.
- Heo, J. and FitzHugh, T. W. (2000). A standardized radiometric normalization method for change detection using remotely sensed imagery. *Photogrammetry Engineering and Remote Sensing*, 66(2).
- Lillesand, T. M. and Kiefer, R.W. (1987). *Remote sensing and image interpretation*. John Wiley, second edition.
- Machado, A. M. C. (1999). *Likelihood Models for Image Registration*. PhD thesis, Universidade Federal de Minas Gerais.
- Maes, F., Collignon, A., Vandermeulen, D., Marchal, G., and Suetens, P. (1997). Multimodality image registration by maximization of mutual information. *IEEE Transactions on Medical Imaging*, 16(2):187–198.
- Markham, B. L. and Barker (1987). Radiometric properties of u. s. processed landsat mss data. *Remote Sensing Environments*, 22:187–208.
- Press, W. H., Flannery, B. P., Teukolsky, S. A., and Vetterling, W. T. (1992). *Numerical Recipes in C*. Cambridge University Press, 2nd edition.
- Queiroz-Neto, J. P. (2001). Registro geométrico e radiométrico automático de imagens landsat na amazônia pela maximização da informação mútua. Master thesis, Universidade Federal de Minas Gerais.
- Samadzadegan, F., Hahn, M., and Hosseini, M. (2003). Ria: Automatic registration of images based on artificial intelligent techniques. In *Proceedings ISPRS Workshop on Challenges in Geospatial Analysis, Integration and Visualization II*.

- Schott, J. R., Salvaggio, C., and Volchok, W. J. (1988). Radiometric scene normalization using pseudoinvariants features. *Remote Sensing Environments*, 26:1–16.
- Shannon, C. E. (1948). A mathematical theory of communication. *Bell Systems Technical Journal*, 27:379–423.
- Song, J., Lu, D., and Wesely, M.L. (2003). A simplified atmospheric correction procedure for the normalized difference vegetation index. *Photogrammetry Engineering and Remote Sensing*, 69(5).
- Trucco, E. and Verri, A. (1998). *Introductory Techniques for 3-D Computer Vision*. Prentice-Hall.
- Viola, P. (1995). *Alignment by Maximization of Mutual Information*. PhD thesis, M.I.T. - Artificial Intelligence Lab.
- Zitova, B. and Flusser, J. (2003). Image registration methods: a survey. *Image and Vision Computing*, 21(11):977–1000.